



Endothelial HIF-1 α Enables Hypothalamic Glucose Uptake to Drive POMC Neurons

Luis Varela,¹ Shigetomo Suyama,¹ Yan Huang,² Marya Shanabrough,¹ Matthias H. Tschöp,³ Xiao-Bing Gao,¹ Frank J. Giordano,² and Tamas L. Horvath^{1,3,4}

Diabetes 2017;66:1511–1520 | <https://doi.org/10.2337/db16-1106>

Glucose is the primary driver of hypothalamic proopiomelanocortin (POMC) neurons. We show that endothelial hypoxia-inducible factor 1 α (HIF-1 α) controls glucose uptake in the hypothalamus and that it is upregulated in conditions of undernourishment, during which POMC neuronal activity is decreased. Endothelium-specific knockdown of HIF-1 α impairs the ability of POMC neurons to adapt to the changing metabolic environment in vivo, resulting in overeating after food deprivation in mice. The impaired functioning of POMC neurons is reversed ex vivo or by parenchymal glucose administration. These observations indicate an active role for endothelial cells in the central control of metabolism and suggest that central vascular impairments may cause metabolic disorders.

The integration of peripheral signals at the level of the arcuate nucleus (Arc) of the hypothalamus is critical for the regulation of energy homeostasis (1,2). Because of its privileged location at the base of the brain and the special configuration that the blood-brain barrier (BBB) presents in this area (3,4), various neuronal populations situated in the Arc are able to sense and respond rapidly to changes in nutritional status (1,2). Two different neuronal populations in the Arc (2,5) are implicated in metabolism regulation: agouti-related protein (AgRP)/neuropeptide Y (NPY) neurons that are activated under negative energy balance and have potent orexigenic effects and proopiomelanocortin (POMC)/cocaine and amphetamine-regulated transcript neurons, which play an antagonistic role to AgRP/NPY and are

activated during energy surplus, thus promoting satiety and energy expenditure.

Nonneuronal cells often have been relegated to a lesser role in the control of complex brain functions. However, the regulation of food intake and energy expenditure is tightly linked to the synaptic plasticity of hypothalamic neural circuits, processes in which glial and endothelial cells also have been implicated (6). In 2010, our group showed the involvement of astrocytes in the modulation of synaptic input onto POMC and AgRP neurons after high-fat diet (HFD) exposure (6). HFD induced reactive gliosis and increased glial coverage of POMC neurons while decreasing synaptic inputs onto POMC cells. Subsequently, our group provided conclusive evidence that astrocytes play direct and autonomous roles in the synaptic plasticity of hypothalamic feeding circuits and related behaviors. In the same study, we showed that HFD exposure triggers plastic changes in the endothelial microvasculature and described an altered morphology of the capillaries of the Arc.

Since having identified the significance of hypothalamic nonneuronal cells (both astrocytes and endothelial cells) in the control of energy homeostasis, a large number of studies have focused on understanding the role these cells play in the control of body weight and food intake (6–8). Two studies from our group and collaborators described the role of leptin and insulin signaling in astrocytes in the control of POMC activity (7,8). Both studies demonstrated the requirement of intact leptin and insulin signaling pathways for a normal response to occur in

¹Program in Integrative Cell Signaling and Neurobiology of Metabolism, Section of Comparative Medicine, Yale University School of Medicine, New Haven, CT

²Department of Medicine, Section of Cardiovascular Medicine, Yale University School of Medicine, New Haven, CT

³Helmholtz Diabetes Center, Helmholtz Zentrum München and Division of Metabolic Diseases, Technische Universität München, Neuherberg, Germany

⁴Department of Anatomy and Histology, University of Veterinary Medicine, Budapest, Hungary

Corresponding authors: Luis Varela, luis.varela@yale.edu, and Tamas L. Horvath, tamas.horvath@yale.edu.

Received 10 September 2016 and accepted 8 March 2017.

This article contains Supplementary Data online at <http://diabetes.diabetesjournals.org/lookup/suppl/doi:10.2337/db16-1106/-/DC1>.

© 2017 by the American Diabetes Association. Readers may use this article as long as the work is properly cited, the use is educational and not for profit, and the work is not altered. More information is available at <http://www.diabetesjournals.org/content/license>.

different energy states (i.e., fasting) and in various hormones and metabolites (i.e., ghrelin, glucose, insulin).

The microvascular endothelium is the functional interface between the blood and tissue compartments and is the final arbiter of nutrient and oxygen delivery. Many metabolic substrates, including glucose, long-chain fatty acids, amino acids, and even nucleotides, cannot efficiently cross the microvascular endothelium without facilitation by specific endothelial transport proteins (9–11), conferring upon the microvasculature the capacity to regulate tissue metabolism by regulation of transendothelial substrate transport. Glucose requires facilitative transport by a membrane protein, *glut1*, to cross the BBB and other microvascular beds. As an illustration of the importance of this mechanism, the genetic mutation of *glut1* in humans causes a clinical syndrome with low cerebrospinal fluid glucose, a propensity for hypoglycemia-induced seizures, and impaired cognition.

The endothelial microvasculature in conjunction with the BBB is involved in the release of blood-borne molecules into the brain (12,13). The BBB contains a special configuration in the medial basal hypothalamus (MBH) and median eminence (ME) that facilitates the entry of blood-borne molecules into this area, although the mechanisms that underlie this process are not well understood. Dynamic changes in the fenestrated capillaries, which are outside the BBB, of the ME have been reported after food deprivation (14). Unlike the BBB microvasculature, fenestrated capillaries do not transport molecules but enable their unfiltered diffusion.

Hypoxia-inducible factor 1 α (HIF-1 α) is a transcription factor that regulates BBB permeability (15) and the expression of many genes involved in angiogenesis, glucose transport (by modulating *glut1* expression), and cellular metabolism, even under normoxic conditions (16,17). HIF-1 α activity is regulated by glucose wherein high glucose concentrations cause increased HIF-1 α activity (15), and we showed that it controls glucose transport from the circulation into tissue parenchyma (17). Previous work has shown that targeted endothelial deletion of HIF-1 α in mice promotes a decrease in *glut1* expression in endothelial cells, which results in increased fasting blood glucose, impaired glucose uptake into brain and heart, abnormal glucose tolerance, and delayed insulin response after intravenous (IV) glucose load (17,18). We hypothesize that this microvascular function of HIF-1 α is critical to the niche microcirculation of the hypothalamus; thus, endothelial HIF-1 α is involved in the regulation of feeding. In the current study, we investigated whether endothelial HIF-1 α is relevant to the control of POMC neurons by glucose.

RESEARCH DESIGN AND METHODS

Animals and Surgery

Mice were kept under standard laboratory conditions with free access to standard chow food and water, unless otherwise stated. The generation of HIF-1 α ^{EC} mice (on a C75BL/6 background) has previously been described

(17,18). HIF-1 α ^{f-f} mice (Cre-negative littermates) were used as controls. For electrophysiological recordings and immunohistochemistry (IHC) staining, HIF-1 α ^{EC} mice were crossed with POMC-GFP or NPY-GFP mice. Body weight was measured weekly, and body composition was performed monthly with the use of magnetic resonance imaging (EchoMRI). Ten- to 12-week-old male mice were used in feeding experiments and all experimental studies. All experimental procedures were performed in accordance with the Yale Animal Resources Center and Institutional Animal Care and Use Committee policies (New Haven, CT).

Intracerebrovascular (ICV) and IV cannulas were implanted at least 4 days before the experiment. Buprenorphine was administered 30 min before surgery, and mice were anesthetized with ketamine. For ICV cannulas, mice were placed in a Kopf stereotaxic instrument that used a platform specifically designed by the manufacturer for mouse surgery. Craniotomy was achieved through the use of a sterile 25-gauge needle; a 33-gauge (sterile) stainless steel, single-guide cannula was placed unilaterally at 1.2 mm lateral and 1 mm posterior from the bregma. Cranioplastic cement and mounting screws were used to fix the cannulas. The incision was closed with a sterile surgical clip. After overnight fasting, mice received an ICV injection of glucose (400 μ g/2 μ L) (19) or saline at the start of the light cycle. For IV cannulas, the left common jugular vein was cannulated by using catheter tubing PE50 (Clay Adams, Parsippany, NJ). After surgery, the incision was closed with a sterile surgical clip. Body temperature and respiratory rate were monitored throughout both procedures. Food and water intake as well as general and cannula appearance were checked 3 days after surgery as part of postoperative care.

Glucose Uptake

Twenty-five micromole per kilogram or 25 nmol of 2-(*N*-[7-nitrobenz-2-oxa-1,3-diazol-4-yl]amino)-2-deoxyglucose (2-NBDG) (Life Technologies), a fluorescent derivative of 2-deoxy-D-glucose (20), were injected by IV and ICV, respectively, and 45 min later, the mice were sacrificed according to Institutional Animal Care and Use Committee protocols. The brains were rapidly removed, frozen in isopentane, and maintained at -40° to -50° C on dry ice before cutting into 20- μ m ($n = 20$) sections. The frozen brain sections of three mice per genotype were thaw-mounted on glass slides and immediately dried on a hot plate at $\sim 60^{\circ}$ C, and fluorescent images were obtained by using a light microscope (Axioplan 2; Zeiss).

Electron Microscopy and Mitochondrial Analysis

The mice ($n = 4$ /group) were anesthetized and perfused (4% paraformaldehyde, 0.1% glutaraldehyde, and 15% picric acid in phosphate buffer [PB]), and their brains were processed for electron microscopic analysis. Ultrathin sections were cut on a Leica Ultramicrotome, collected on Formvar-coated single-slot grids, and analyzed with a Tecnai 12 BioTWIN electron microscope (FEI). Analysis of mitochondria (area, coverage, density, and contact with the endoplasmic reticulum [ER]) was performed in an unbiased fashion, as previously described (21,22).

IHC

Mice (at least five per group in all the experiments) were anesthetized and perfused (4% paraformaldehyde, 0.1% glutaraldehyde, and 15% picric acid in PB). Brains were kept at 4°C in 4% paraformaldehyde for 24 h after which time they were washed with PB, and 50- μ m sections of the specific Arc area were cut. Sections were pretreated with 0.2% Triton for 30 min before the primary antibodies. Sections were incubated overnight at room temperature in either c-Fos (Millipore), platelet endothelial cell adhesion molecule (PECAM) (BD Biosciences), or HIF-1 α (Novus Biologicals). Samples were then washed three times with PB and incubated with the corresponding secondary antibody (Alexa Fluor; Invitrogen) for 1 h, after which they were mounted on precleaned microscope slides (Thermo Fisher Scientific) with fluorescent mounting medium (Dako). Pictures were taken with a confocal microscope (Olympus). c-Fos activation, POMC neuron-vessel contacts, and vessel length were analyzed through an FV10-ASW 4.0 Viewer.

Western Blot

Mice ($n = 4$ –5/group) were sacrificed, and the MBH was extracted. Protein b was extracted by using radioimmunoprecipitation assay buffer containing cOmplete Protease Inhibitor Cocktail (Roche). Proteins were transferred on polyvinylidene fluoride membranes by using a Trans-Blot Turbo transfer apparatus (Bio-Rad, Hercules, CA) and incubated with anti-HIF-1 α (1:1,000; Novus Biologicals) and anti-GAPDH (1:10,000; Calbiochem). Detection was carried out with enhanced chemiluminescence (Bio-Rad).

RNA Preparation and Quantitative Real-time PCR

Mice (at least six per group in all experiments) were sacrificed, and the MBH was extracted and kept in RNAlater (QIAGEN) for 2 days. Total RNA was extracted from the MBH according to the TRI Reagent protocol, and cDNA was then synthesized from total RNA by using a high-capacity cDNA reverse transcription kit (QIAGEN). Real-time PCR was performed as previously described (21). All probes were purchased from Applied Biosystems.

Electrophysiology

Whole-cell recordings were made from POMC-GFP/HIF-1 α ^{EC} mice or their respective controls. Hypothalamic coronal slices (300 μ m) containing the Arc were maintained at 33°C and perfused with artificial cerebrospinal fluid (in mmol/L: NaCl 124; KCl 3, CaCl₂ 2, MgCl₂ 2, NaHCO₃ 26, NaH₂PO₄ 1.23, glucose 3, pH 7.4) and NaOH and was continuously bubbled with 5% CO₂ and 95% O₂. In the brain sections, POMC neurons were patched after a gigaohm seal. To rapidly apply and remove glutamate to (and from) the recorded neurons, a droplet of artificial cerebrospinal fluid containing glutamate (400 μ mol/L) was applied to the bath solution at a distance of \sim 500 μ m from the recorded neurons. Miniature excitatory postsynaptic current (mEPSC) and miniature inhibitory postsynaptic current (mIPSC) were monitored in control conditions. The pipette solution contained (in mmol/L) gluconic acid 140,

CaCl₂ 1, MgCl₂ 2, EGTA 1, HEPES 10, Mg-ATP 4, and Na₂-GTP 0.5, pH 7.3 with KOH. All data were sampled at 3–10 kHz and filtered at 1–3 kHz with an Apple Macintosh computer running AxoGraph 4.9 software (Axon Instruments). Electrophysiological data were analyzed with AxoGraph 4.9 and plotted with Igor Pro software (WaveMetrics, Lake Oswego, OR).

Statistical Analysis

All data are expressed as mean \pm SEM. The means between groups were analyzed by Student *t* test. For analyses of more than two groups and two genotypes, a two-way ANOVA was used followed by Bonferroni post hoc test, unless otherwise stated. Significance for all analyses was taken at $P < 0.05$, $P < 0.01$, and $P < 0.001$. Shapiro-Wilk normality test was used to assess the Gaussian distribution of each data set. All data sets showed normal distribution.

RESULTS

Loss of Endothelial HIF-1 α Specifically Regulates POMC Neurons in the Arc

Mice lacking HIF-1 α were previously described to show impaired glucose uptake in various peripheral tissues as well as in the brain (17). Moreover, despite the impairment in glucose uptake, these mice exhibit higher fasting glucose levels and delayed glucose clearance. Given these facts, we checked whether this altered glucose homeostasis driven by HIF-1 α affects the various neuronal populations within the Arc. To confirm the previous data, we first checked whether glucose uptake is also altered specifically within the MBH. We treated transgenic and control mice IV with 2-NBDG (a fluorescent derivative of 2-deoxy-D-glucose). We found that HIF-1 α ^{EC} mice showed less labeled glucose in the Arc relative to their controls (Fig. 1A). Both POMC and AgRP neurons have been widely described as glucose sensitive. They respond and change their activity and synaptic organization depending on the glucose concentration. Of note, we found POMC mRNA levels to be significantly lower in HIF-1 α ^{EC} mice (Fig. 1B), whereas no differences were found in AgRP or NPY mRNA expression (Fig. 1B). POMC neuronal activity level (assessed by c-Fos expression) was also significantly lower in HIF-1 α ^{EC} mice compared with the values of control littermates (Fig. 1C and E). No differences were found in AgRP activation in the fed state (Fig. 1D and F). In line with previous studies, we did not find any change in vascularization within the Arc as assessed by mRNA vascular endothelial growth factor (VEGF) levels and IHC against PECAM (Fig. 1G–I). Of note, we found that contact between microvessels (PECAM-positive) and POMC neurons were significantly higher in HIF-1 α ^{EC} mice than in controls (Supplementary Fig. 1A and B), indicating a structural adaptation of the Arc likely related to the fundamental dependence of POMC neurons on glucose. Taken together, these results indicate that glucose uptake in the Arc is mediated by HIF-1 α –controlled endothelial transport and modulates POMC neurons specifically.

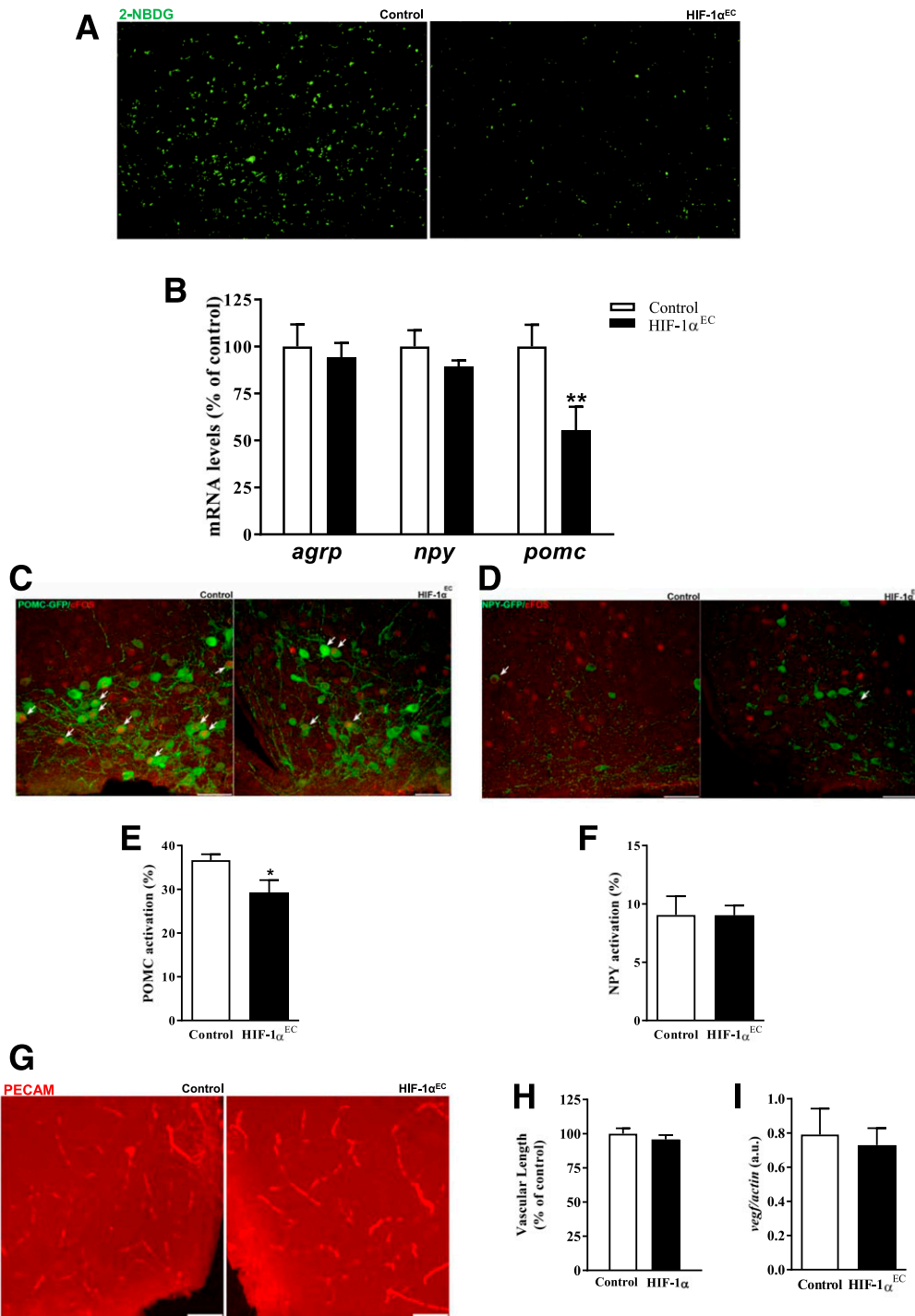


Figure 1—Impaired glucose uptake in the Arc leads to a loss of function in POMC neurons. *A*: Representative images of the Arc after IV administration of 2-NBDG (green). *B*: Expression levels of *AgRP*, *NPY*, and *POMC* from the MBH of ad libitum fed wild-type and HIF-1 α^{EC} mice. *C* and *D*: Representative images of c-Fos (red) activation in POMC/*NPY* (green) neurons. Arrows indicate double-labeled cells (POMC/*NPY*-cFOS). *E* and *F*: Quantification of c-Fos activation in POMC and *NPY* neurons, respectively. *G*: Immunofluorescence of PECAM (endothelial marker) in the Arc of control and HIF-1 α^{EC} mice. *H*: Total length of vessel stained with PECAM from the MBH. *I*: Expression levels of VEGF from the MBH of ad libitum fed control and HIF-1 α^{EC} mice. Scale bars = 50 μ m. **P* < 0.05, ***P* < 0.01. a.u., arbitrary units.

Impaired Transendothelial Glucose Uptake Controls Synaptic Organization and Mitochondrial Network of POMC Neurons

That POMC neurons show different synaptic patterns depending on energy status is well known. Energy deficiency is

associated with a decrease in the number of excitatory synapses and an increase of inhibitory synapses. Therefore, we investigated whether this disrupted hypothalamic glucose uptake is associated with changes in the synaptic organization of POMC neurons through electrophysiological

studies. No changes were found in the frequency of mEPSC and mIPSC between POMC neurons of control and transgenic mice (Fig. 2A and C). Of note, we found that this set of neurons exhibits an altered amplitude of both the mEPSC and the mIPSC (Fig. 2B and D). The mEPSC events displayed a smaller amplitude in HIF-1 α mice (Fig. 2B), whereas the mIPSCs presented an increased amplitude. These electrophysiological data support our previous findings about POMC activation. Diminished excitatory and increased inhibitory input onto POMC cells could be the cause of the baseline inactivation of these cells.

Changes in systemic metabolism induces changes in mitochondrial function and dynamics in AgRP and POMC neurons (21,22). To determine whether mitochondria are affected by a reduction of glucose uptake in the Arc, we carried out electron microscopic analysis on the POMC neurons of HIF-1 α ^{EC} mice and their control littermates. We found that in HIF-1 α ^{EC} mice, mitochondrial coverage per cell was decreased (Fig. 3A and B), which is in accordance with previous results that showed that in a fasted state (marked by low glucose availability), this parameter is decreased in POMC neurons (21,22). Similarly, we also observed more rounded mitochondria in HIF-1 α ^{EC} mice than in the controls (21,22) (Fig. 3C and D). We and others have shown that mitofusin-1 and -2 (*mfn1/2*) play critical roles in mitochondrial fusion and in the interaction between mitochondria and ER. Alterations in the association between these two organelles are linked to metabolic shifts. Furthermore, we found in HIF-1 α ^{EC} mice a lower frequency of mitochondria-ER contacts than in controls (Fig. 3E), which is in line with the fact that expression of *mfn1/2* was also lower in HIF-1 α ^{EC} mice (Fig. 3F and G). Together, these results indicate a dependence of POMC neurons on transendothelial glucose transport.

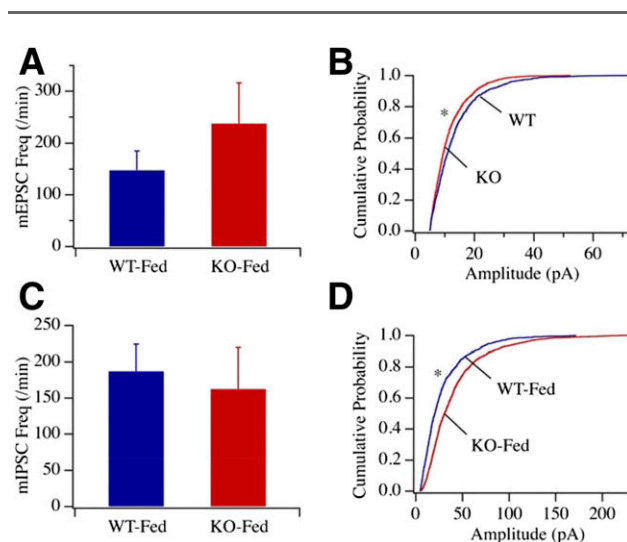


Figure 2—POMC neurons show changed synaptic organization in HIF-1 α ^{EC} mice. Electrophysiological recordings showing frequency and amplitude of mEPSC (A and B) and mIPSC (C and D) onto POMC neurons from HIF-1 α ^{EC} mice and their control littermates. * $P < 0.05$. Freq, frequency; KO, knockout; WT, wild type.

HIF-1 α ^{EC} Mice Exhibit Altered Response to Fasting

Despite the above alterations in POMC neuronal parameters and function in HIF-1 α ^{EC} mice, we did not observe significant differences in body weight, body composition, or food intake under baseline conditions (Fig. 4A and B and Supplementary Fig. 2A and B). With the aim of determining whether hypothalamic HIF-1 α is involved in response to changes in the nutritional state of the mice, we analyzed the protein expression levels of HIF-1 α in Arc lysates of wild-type mice under fed and fasted conditions. We found that after a 24-h fast, HIF-1 α levels were increased (Fig. 4C). Next, we tested the feeding behavior of HIF-1 α ^{EC} mice after food deprivation, a state associated with low glucose availability in the MBH (23). We observed a significantly elevated increase in food intake in HIF-1 α ^{EC} mice after fasting relative to controls (Fig. 4D). Consistent with the above data on AgRP mRNA of ad libitum fed mice, HIF-1 α ^{EC} mice showed the expected response to fasting in AgRP mRNA expression, but POMC levels remained unchanged compared with the fed state (Fig. 4E and F). As expected, control mice had increased levels in AgRP expression and decreased levels in POMC after fasting (Fig. 4E and F). This loss in POMC expression was also accompanied by significantly lower POMC neuronal activation as assessed by analysis of *c-Fos* activation (Fig. 4G and H). Furthermore, because glucose levels are altered after fasting and POMC neurons showed electrophysiological changes during this negative energy state, we studied whether endothelial HIF-1 α ^{EC} affects electrophysiological properties. As described above, loss of endothelial HIF-1 α decreases the amplitude of excitatory events and increases the amplitude of inhibitory events onto the POMC neurons. After fasting, we found that POMC neurons in HIF-1 α ^{EC} mice showed an increased amplitude of mEPSC, with no differences detected in mIPSC (Fig. 4I–L). The findings show that endothelial HIF-1 α plays a crucial role in the cellular adaptations of POMC neurons to the fasting state, which affects feeding behavior of mice by modulating excitatory inputs onto this neuronal population.

POMC Neurons Remain Glucose Sensitive in HIF-1 α ^{EC} Mice

All the results described above indicate that endothelial HIF-1 α plays a key role in the modulation of POMC activity. However, we wanted to address whether parenchymal glucose levels rather than other cellular events underlie the differential phenotype of these neurons *in vivo* in HIF-1 α ^{EC} mice. We administered glucose ICV after fasting, which has a rapid, short-term effect on neuropeptide expression (19). We found that food intake differences between transgenic and control mice were abolished (Fig. 5A). In line with this finding, POMC levels in HIF-1 α ^{EC} mice also became indistinguishable from that of control animals (Fig. 5C). No major changes were found in AgRP mRNA levels after glucose administration in both control and transgenic mice (Fig. 5B). Furthermore, POMC neurons appeared to be even more sensitive to ICV glucose administration (Fig. 5C).

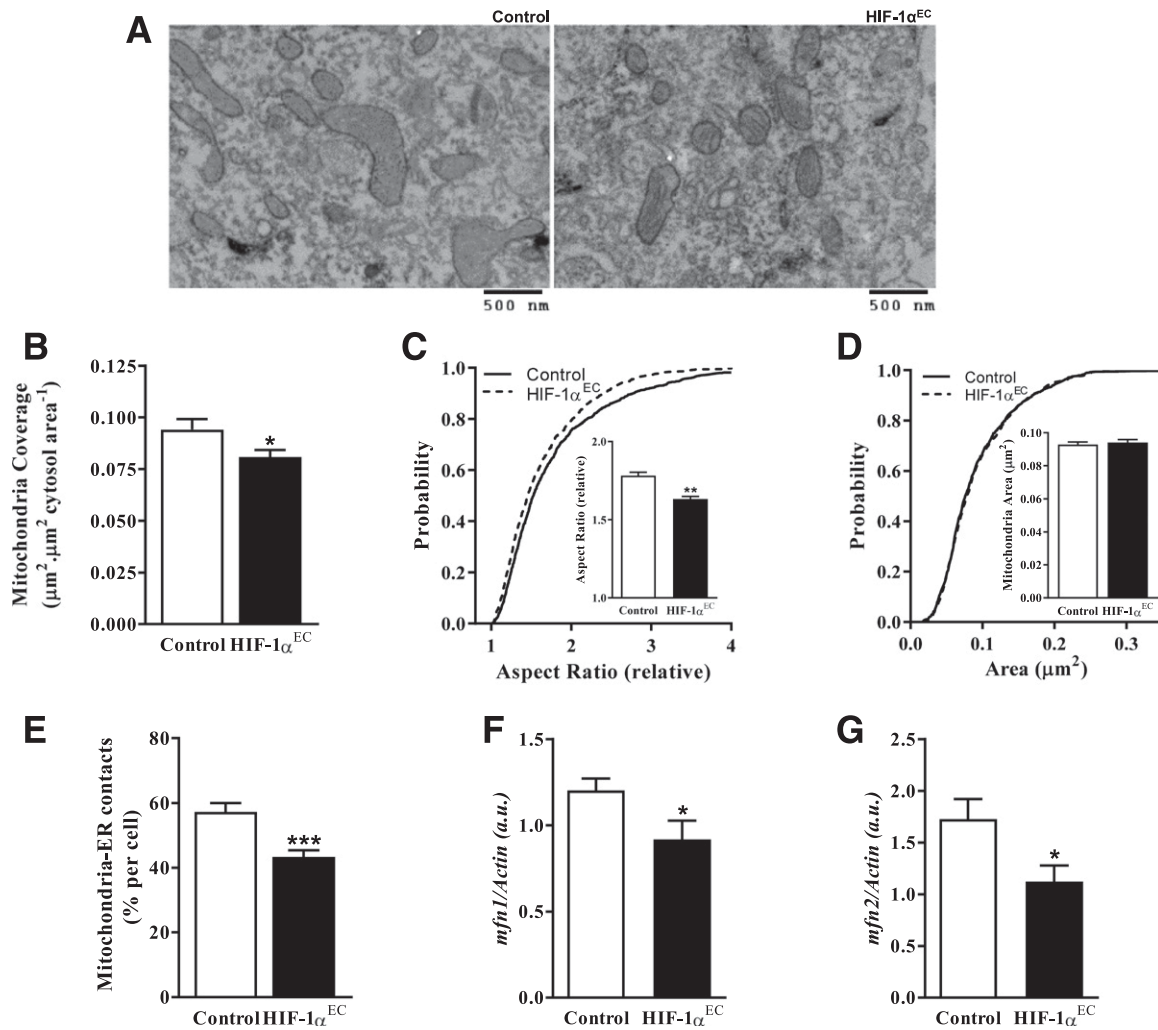


Figure 3—Mitochondrial network is altered in POMC neurons of HIF-1 α^{EC} mice. **A**: Representative electron micrographs of mitochondria profiles in POMC neurons from HIF-1 α^{EC} mice and their control littermates. **B**: Mitochondria coverage in POMC neurons of HIF-1 α^{EC} mice and their control littermates. **C**: Cumulative distribution and mean of mitochondria aspect ratio from ad libitum fed HIF-1 α^{EC} mice and their control littermates. **D**: Cumulative distribution and mean of mitochondria area from ad libitum fed HIF-1 α^{EC} mice and their control littermates. **E**: Percentage of mitochondria in direct contact with the ER per cell. **F** and **G**: Expression levels of *mfn1* and *mfn2* from the MBH of HIF-1 α^{EC} mice and their control littermates fed ad libitum. * $P < 0.05$, ** $P < 0.01$, *** $P < 0.001$. a.u., arbitrary units.

HIF-1 α^{EC} mice presented raised levels of POMC mRNA compared with their control littermates. To confirm that this ICV treatment results in equal availability of glucose in transgenic and control mice, we also injected 2-NBDG ICV. We found no differences in signal, specifically in the Arc, between transgenic and control mice (Fig. 5D and E). In line with these observations, mitochondrial analysis revealed greater effects on mitochondria area in HIF-1 α^{EC} mice than in their controls (Fig. 5F and G) after ICV glucose injection.

Finally, to confirm that POMC neurons are still sensitive to parenchymal glucose, we carried out electrophysiological studies by using various glucose concentrations. POMC neurons of HIF-1 α^{EC} mice showed the same response as control mice, as assessed by action potentials (Fig. 5H and I). Despite the loss of activity on the part of the POMC neurons

in this model, we found that these neurons are still able to respond to parenchymal glucose load.

DISCUSSION

During the past decade, an increasing amount of effort has been put forth to understand the basis of energy homeostasis regulation, and that control of food intake and energy expenditure occurs at a central level is now known. Hormones, nutrients, and other factors transported by the blood from peripheral tissues provide information about current energy status to different areas of the central nervous system, and these signals are integrated mainly in the hypothalamus (1). The hypothalamus is especially sensitive to changes in nutritional status, because of its privileged location at the base of the brain as well as its unique configuration with the BBB (3,4). Within the hypothalamus,

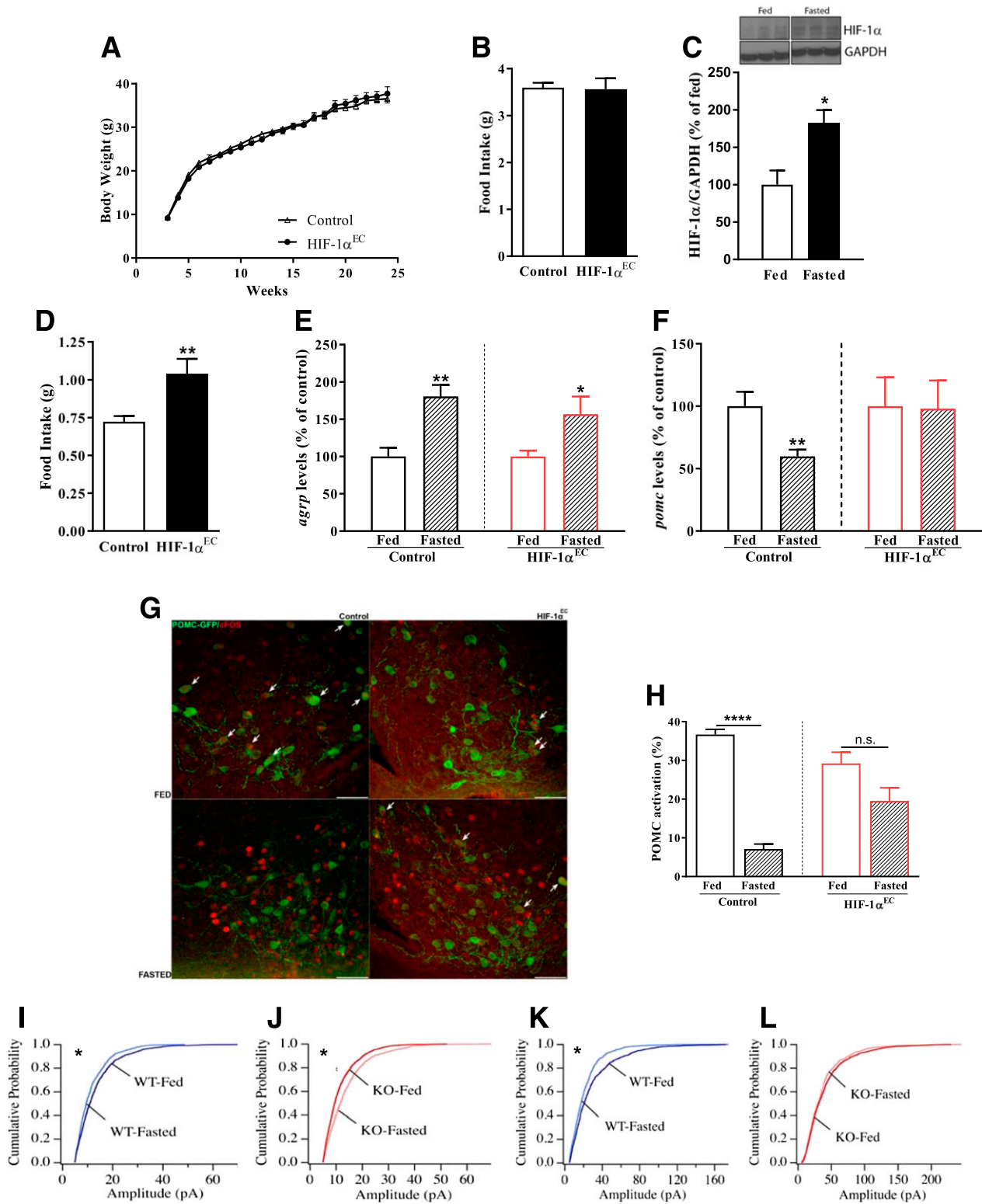


Figure 4—Feeding behavior is unaltered in the fed state but displays changes after fasting. *A* and *B*: Body weight and daily food intake in 10- to 12-week-old HIF-1 α^{EC} mice and their control littermates fed ad libitum. *C*: HIF-1 α levels (representative Western blot images and quantification) from MBH of fed and fasted mice. *D*: Food intake (2 h) after overnight fasting. *E* and *F*: Expression levels of AgRP and POMC from MBH of fasted HIF-1 α^{EC} mice and their control littermates. *G*: Representative images of c-Fos (red) activation in POMC (green) neurons. Arrows indicate double-labeled cells (POMC-cFOS). *H*: Quantification of c-Fos activation from fasted HIF-1 α^{EC} and their respective controls. *I* and *J*: Amplitude of mEPSC onto POMC neurons from control and HIF-1 α^{EC} mice, respectively, in the fed and fasted condition. *K* and *L*: Amplitude of mIPSC onto POMC neurons from control and HIF-1 α^{EC} mice, respectively, in the fed and fasted condition. Scale bars = 50 μ m. * P < 0.05, ** P < 0.01, **** P < 0.0001. KO, knockout; n.s., not significant; WT, wild type.

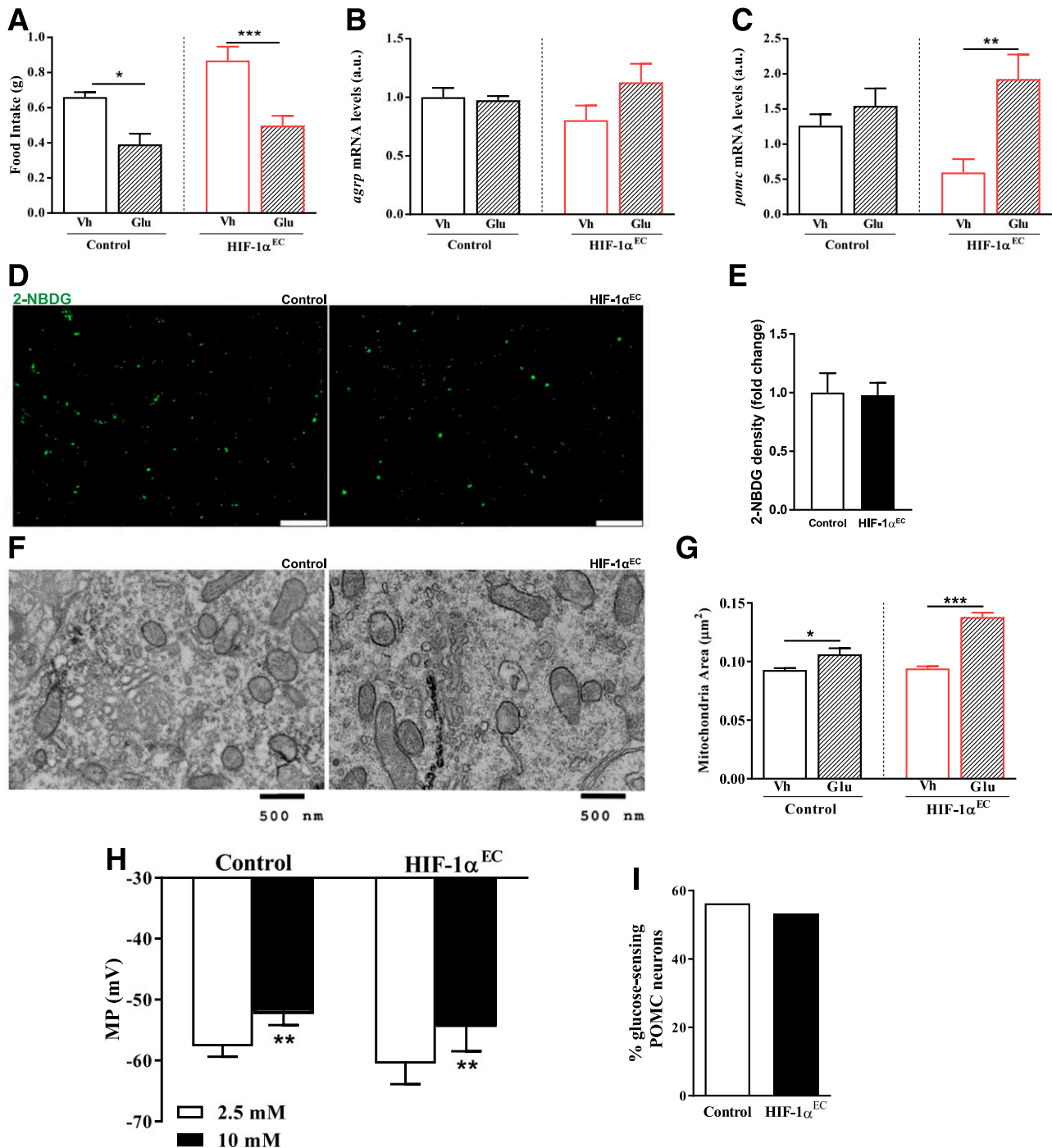


Figure 5—ICV glucose administration provokes alterations on POMC neurons. **A**: Food intake (2 h) after ICV glucose administration of fasted wild-type and HIF-1 α^{EC} mice. **B**: AgRP levels from the MBH of HIF-1 α^{EC} and control mice after acute central administration of glucose or saline. **C**: POMC levels from the MBH of HIF-1 α^{EC} and control mice after acute central administration of glucose or saline. **D** and **E**: Representative images of the Arc after ICV administration of 2-NBDG (green) and their quantification. Scale bars = 50 μm . **F**: Representative electron micrographs of mitochondria profiles in POMC neurons from HIF-1 α^{EC} mice and their control littermates after acute ICV glucose administration. **G**: Mitochondria area of HIF-1 α^{EC} and control mice after acute administration of glucose or saline in the fed state. **H**: Membrane potential (MP) from POMC neurons of HIF-1 α^{EC} and control mice exposed to various glucose concentrations. **I**: Percentage of POMC neurons activated by glucose. * $P < 0.05$, ** $P < 0.01$, *** $P < 0.001$. a.u., arbitrary units; Glu, glucose; Vh, vehicle.

the Arc contains the AgRP (responsible for orexigenic tone) and the POMC (anorexigenic tone) neurons, which are located on different sides of the BBB (24). The endothelial microvasculature that forms the BBB is modulated

by blood glucose availability, and HIF-1 α has been shown to be a major regulator of glucose throughout the brain (17). Thus, this protein may be important for the regulation of feeding behavior. However, the means by which

glucose is trafficked between the bloodstream and the Arc remains unclear. Our goal in the current study was to gain a better understanding of glucose transport throughout the microvasculature in both POMC and AgRP neurons in the Arc.

By using a well-established animal model for GLUT1 downregulation in the endothelium, the HIF-1 α ^{EC} mouse (17,18), we report a differential dependency on the part of the POMC and AgRP neurons with regard to glucose transport through the vessels in a manner that perhaps depends on the location of the two neuronal populations with respect to the BBB. The AgRP neurons remain unchanged in the basal state or in response to fasting in HIF-1 α ^{EC} mice compared with their littermates, whereas POMC neurons appear to be inactivated. mRNA, c-Fos activation, and electrophysiological and mitochondrial parameters provide evidence that a loss of function occurring in the POMC neurons, in both a fed and a fasted state, promotes altered feeding behavior. Because partial disruption of vascular glucose transport affected POMC neurons only, the principal source of glucose uptake into the POMC neurons may come through transport across the BBB. To determine whether the loss of response of POMC neurons was due to a complete inactivation of these neurons or caused by impaired glucose uptake from the BBB, we administered ICV glucose and found that it blocked food intake after fasting in wild-type and knockout mice to the same degree. This result, together with the observation of increased POMC mRNA levels and electron microscopic data, indicates that POMC neurons are still sensitive to the glucose that reaches the Arc and that their loss of function is due to impaired glucose transport across the BBB.

Although both POMC and AgRP neurons are glucose sensitive (25), AgRP neurons have been described to be located outside the BBB and are in proximity to the third ventricle and ME. These neurons can sense changes in blood glucose directly through the fenestrated capillaries of the ME by diffusion and, thus, do not need to rely on glucose transport across the BBB, as is necessary for POMC neurons. Accordingly, in the current study, we found that AgRP neurons were unaffected by chronic low-glucose levels in the Arc; the AgRP neurons are able to sense the high blood glucose levels because of their proximity with the fenestrated capillaries that diffuse different molecules and factors into the hypothalamus regardless of endothelial transport.

Despite this loss of function on the part of the POMC neurons, why HIF-1 α ^{EC} mice have increased refeeding remains unclear. After fasting, POMC levels (mRNA and activation) remain unchanged; thus, HIF-1 α ^{EC} mice should have decreased feeding, which could be explained by a plastic remodeling during the developmental stage that changes neuronal circuitry. To address this question, more effort is required. A postnatal ablation of HIF-1 α in endothelial cells would be necessary to completely unmask the true role of transendothelial glucose transport in the control of POMC activity and acute response to fasting.

The impact of a transendothelial impaired glucose uptake on POMC neurons is a novel finding that highlights the role of the BBB in correct nutrient sensing. The observations that an endothelium-specific knockdown of HIF-1 α apparently did not affect orexigenic-promoting AgRP neurons but impaired the ability of anorexigenic-promoting POMC neurons to adapt to changes in glucose levels and that these neurons were functionally identical to wild-type neurons suggest that glucose transport across the BBB is impaired in these mice. These findings highlight the critical role of the endothelial cells in the control of satiety and identify brain vascular-related mechanisms as novel targets for the treatment of metabolic disorders.

Funding. This study received funding from the Helmholtz Alliance ICEMED – Imaging and Curing Environmental Metabolic Diseases (to M.H.T. and T.L.H.); funding from the Institute for Advanced Study of Technische Universität München (IAS-TUM) (Hans-Fischer Senior Fellowship to T.L.H.); and funding to M.H.T. from the Alexander von Humboldt Foundation, the Helmholtz Alliance ICEMED, and the Helmholtz Initiative on Personalized Medicine iMed by Helmholtz Association, as well as from the German Research Foundation (DFG) (SFB1123), the DFG Nutripathos Project ANR-15-CE14-0030, and the European Research Council (ERC) (AdG HypoFlam no. 695054). This study was also supported by a DRC Pilot Project grant from the National Institutes of Health (P30-DK-045735 to F.J.G.) and a research grant from the Klarman Family Foundation (to T.L.H.).

Duality of Interest. No potential conflicts of interest relevant to this article were reported.

Author Contributions. L.V. and T.L.H. designed the experiments and wrote the manuscript. L.V., S.S., Y.H., and X.-B.G. performed the experiments. M.S. provided technical support. M.H.T. and F.J.G. edited the manuscript and provided intellectual support. T.L.H. is the guarantor of this work and, as such, had full access to all the data in the study and takes responsibility for the integrity of the data and the accuracy of the data analysis.

References

- Williams KW, Elmquist JK. From neuroanatomy to behavior: central integration of peripheral signals regulating feeding behavior. *Nat Neurosci* 2012;15:1350–1355
- Varela L, Horvath TL. Leptin and insulin pathways in POMC and AgRP neurons that modulate energy balance and glucose homeostasis. *EMBO Rep* 2012;13:1079–1086
- Ferguson AV. Circumventricular organs: integrators of circulating signals controlling hydration, energy balance, and immune function. In *Neurobiology of Body Fluid Homeostasis: Transduction and Integration*. De Luca LA, Menani JV, Johnson AK, Eds. Boca Raton, FL, CRC Press, 2014, p. 23–36
- Sisó S, Jeffrey M, González L. Sensory circumventricular organs in health and disease. *Acta Neuropathol* 2010;120:689–705
- Belgardt BF, Okamura T, Brüning JC. Hormone and glucose signalling in POMC and AgRP neurons. *J Physiol* 2009;587:5305–5314
- Horvath TL, Sarman B, García-Cáceres C, et al. Synaptic input organization of the melanocortin system predicts diet-induced hypothalamic reactive gliosis and obesity. *Proc Natl Acad Sci U S A* 2010;107:14875–14880
- García-Cáceres C, Quarta C, Varela L, et al. Astrocytic insulin signaling couples brain glucose uptake with nutrient availability. *Cell* 2016;166:867–880
- Kim JG, Suyama S, Koch M, et al. Leptin signaling in astrocytes regulates hypothalamic neuronal circuits and feeding. *Nat Neurosci* 2014;17:908–910
- Olson AL, Pessin JE. Structure, function, and regulation of the mammalian facilitative glucose transporter gene family. *Annu Rev Nutr* 1996;16:235–256

10. Glatz JF, Luiken JJ, Bonen A. Membrane fatty acid transporters as regulators of lipid metabolism: implications for metabolic disease. *Physiol Rev* 2010;90:367–417
11. Mann GE, Yudilevich DL, Sobrevia L. Regulation of amino acid and glucose transporters in endothelial and smooth muscle cells. *Physiol Rev* 2003;83:183–252
12. Ben-Zvi A, Lacoste B, Kur E, et al. Mfsd2a is critical for the formation and function of the blood-brain barrier. *Nature* 2014;509:507–511
13. Nguyen LN, Ma D, Shui G, et al. Mfsd2a is a transporter for the essential omega-3 fatty acid docosahexaenoic acid. *Nature* 2014;509:503–506
14. Langlet F, Levin BE, Luquet S, et al. Tanycytic VEGF-A boosts blood-hypothalamus barrier plasticity and access of metabolic signals to the arcuate nucleus in response to fasting. *Cell Metab* 2013;17:607–617
15. Yan J, Zhang Z, Shi H. HIF-1 is involved in high glucose-induced paracellular permeability of brain endothelial cells. *Cell Mol Life Sci* 2012;69:115–128
16. Huang Y, Hickey RP, Yeh JL, et al. Cardiac myocyte-specific HIF-1alpha deletion alters vascularization, energy availability, calcium flux, and contractility in the normoxic heart. *FASEB J* 2004;18:1138–1140
17. Huang Y, Lei L, Liu D, et al. Normal glucose uptake in the brain and heart requires an endothelial cell-specific HIF-1 α -dependent function. *Proc Natl Acad Sci U S A* 2012;109:17478–17483
18. Tang N, Wang L, Esko J, et al. Loss of HIF-1alpha in endothelial cells disrupts a hypoxia-driven VEGF autocrine loop necessary for tumorigenesis. *Cancer Cell* 2004;6:485–495
19. Cha SH, Wolfgang M, Tokutake Y, Chohan S, Lane MD. Differential effects of central fructose and glucose on hypothalamic malonyl-CoA and food intake. *Proc Natl Acad Sci U S A* 2008;105:16871–16875
20. Itoh Y, Abe T, Takaoka R, Tanahashi N. Fluorometric determination of glucose utilization in neurons in vitro and in vivo. *J Cereb Blood Flow Metab* 2004;24:993–1003
21. Dietrich MO, Liu ZW, Horvath TL. Mitochondrial dynamics controlled by mitofusins regulate AgRP neuronal activity and diet-induced obesity. *Cell* 2013;155:188–199
22. Schneeberger M, Dietrich MO, Sebastián D, et al. Mitofusin 2 in POMC neurons connects ER stress with leptin resistance and energy imbalance. *Cell* 2013;155:172–187
23. Dunn-Meynell AA, Sanders NM, Compton D, et al. Relationship among brain and blood glucose levels and spontaneous and glucoprivic feeding. *J Neurosci* 2009;29:7015–7022
24. Olofsson LE, Unger EK, Cheung CC, Xu AW. Modulation of AgRP-neuronal function by SOCS3 as an initiating event in diet-induced hypothalamic leptin resistance. *Proc Natl Acad Sci U S A* 2013;110:E697–E706
25. Claret M, Smith MA, Batterham RL, et al. AMPK is essential for energy homeostasis regulation and glucose sensing by POMC and AgRP neurons. *J Clin Invest* 2007;117:2325–2336